A Genetically Targetable Fluorescent Probe of Channel Gating with Rapid Kinetics

Kazuto Ataka and Vincent A. Pieribone
The John B. Pierce Laboratory, Interdepartmental Neuroscience Program, Department of Cellular and Molecular Physiology, Yale University School of Medicine, New Haven, Connecticut 06519 USA

ABSTRACT We have developed a genetically targetable, optical channel-gating reporter that converts rapid membrane potential changes into changes in fluorescence intensity. We have named this construct SPARC (sodium channel protein-based activity reporting construct). Green fluorescent protein was inserted into an intracellular loop of a reversibly nonconducting form of the rat μI skeletal muscle voltage-gated sodium channel. Rapid changes of the membrane potential modulate the fluorescence of the inserted green fluorescent protein. This change in fluorescence can faithfully report depolarizing pulses as short as 2 ms. The fluorescence signal does not inactivate during extended depolarizations. Several features of the probe's response properties indicate that it likely reports gating charge movement of a single domain of rat μI skeletal muscle. This probe provides a new approach for studying rapid channel movements and may possibly act as a fluorescent activity reporter in excitable cells.

INTRODUCTION

Voltage-gated channels are essential proteins for the functioning of excitable tissues. A major outstanding question is what sort of conformational changes occur in channel structure in response to membrane potential changes. Targeted tagging of a fluorescent molecule combined with fluorescence resonance energy transfer (FRET) measurements provides a novel way to study rapid conformational changes in a channel by optical methods (Cha et al., 1999b; Glauner et al., 1999). However, this technique is not necessarily suitable for studying channel kinetics in vivo.

The recent development of a fluorescent protein construct (FlaSh) based on the insertion of green fluorescent protein (GFP) into a nonconducting mutant of the shaker K^+ channel represents a promising approach to study conformational changes in a channel protein (Siegel and Isacoff, 1997). Upon depolarization, cells expressing FlaSh undergo a reduction in fluorescent intensity. As suggested by its slow kinetics (τ_{off} >85 ms), the fluorescence change derived from FlaSh is likely coupled to C-type inactivation of the GFP-tagged potassium channel. This work also suggests the possibility of studying electrical activity in excitable cells by genetic introduction of such a probe. Although this approach seems promising, the FlaSh probe is unfortunately too slow to follow action potentials and may alter a cell's physiology if expressed in neurons, as it is likely to co-assemble with native channel subunits.

We report a novel protein-based optical probe that is capable of reporting the rapid kinetics of a voltage-gated channel as changes in a fluorescence signal. This probe provides a new approach to study the rapid conformational changes associated with gating of a sodium channel. In addition, this probe could potentially be used as a genetically targetable electrical activity marker.

Received for publication 14 June 2001 and in final form 18 September 2001.

Address reprint requests to Dr. Vincent A. Pieribone, John B. Pierce Laboratory, Yale School of Medicine, New Haven, CT 06519. Tel.: 203-562-9901; Fax: 203-624-4950; E-mail: vincent.pieribone@cmp.yale.edu.

0006-3495/02/01/509/08 $2.00

MATERIALS AND METHODS

Making of a mammalianized wild-type GFP (E-wtGFP)

pEGFP vector (BD Biosciences Clontech, Palo Alto, CA) was used as a template to reverse-mutate EGFP back to wild-type GFP by introducing a T65S and L64F mutation into EGFP. This polymerase chain reaction (PCR) fragment (full-length E-wtGFP) was subcloned into the zero-blunt vector (Invitrogen Life Technologies, Carlsbad, CA), then sequenced to confirm the mutations. The E-wtGFP sequence was further subcloned into pTYB11 expression vector and recombinant protein was purified by the IMPACT-CN kit (New England Biolabs, Beverly, MA). The purified E-wtGFP recombinant protein was confirmed to have the known spectrum of the wild-type GFP (Ward, 1998) by a scanning spectrofluorometer (Fig. 3 *A*; SPEX Industries, Edison, NJ).

Insertion of GFP into the sodium channel sequence

A reversible pore mutant of the rat μI skeletal sodium channel (rSkM1; $rNa_v1.4$) in the pSP64T vector was kindly provided by Dr. Eduardo Marban (Johns Hopkins University, Baltimore, MD) (Perez-Garcia et al., 1997). A total of 10 different insertion sites (after residues: P22, D500, L850, K1334, I1430, S1436, D1621, K1718, E1789, V1840) were tested, mostly in cytoplasmic loops (Fig. 1 *A*). Insertions were carried out by first introducing a unique restriction site (Asc I) into the sodium channel sequence, then the AscI-flanked sequence of GFP, lacking a termination codon, was inserted.

For the production of the construct SPARC (*S*odium channel *P*rotein-based *A*ctivity *R*eporting *C*onstruct), an AscI-containing nine base-pair sequence (AGGCGCGCC) was first introduced in-frame between L850 and S851 of the sodium channel. AscI containing 5′ and 3′ pieces were amplified by PCR. The 5′ piece was then digested by AscI and BsiWI (both from New England Biolabs). The 3′ piece was also digested by AscI and BstZ17I (New England Biolabs). These two fragments were subcloned into the zero-blunt vector and were then digested with AscI and BsiWI for the

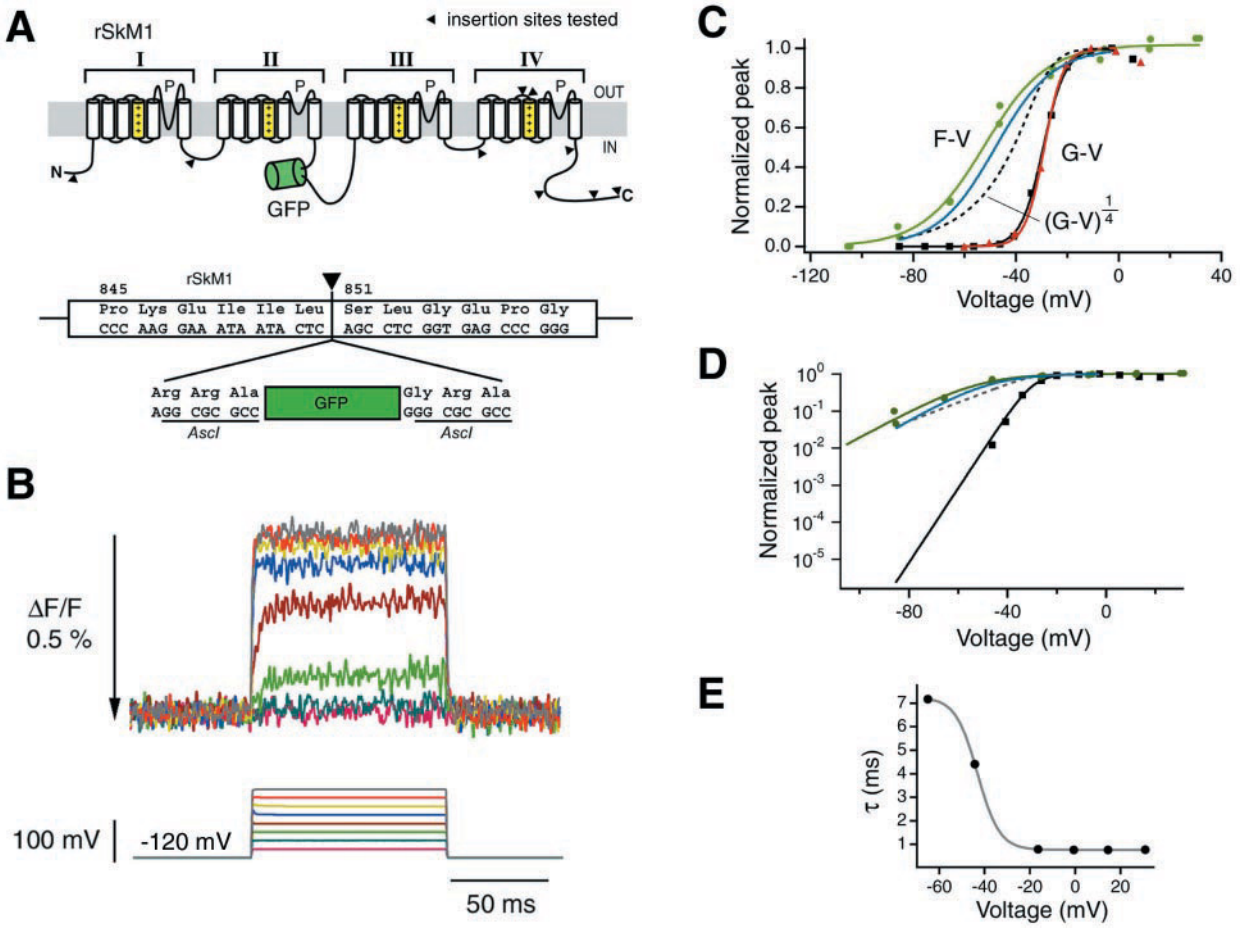

FIGURE 1 Structure and voltage response of the SPARC probe. (*A*) Schematic representation of the SPARC probe. The GFP sequence (*green*) was inserted between L850 and S851 of the rat μ1 skeletal muscle sodium channel. The channel consists of four repeats of six transmembrane domains which each contain a pore lining region (P) and a positively charged mobile transmembrane segment (S4; *yellow* with + charges). The arrowheads indicate nine other sites where insertions of GFP were tested. (*B*) Fluorescence signal (*top*) from an oocyte during progressively greater depolarizing voltage steps (*lower*). Each fluorescence trace represents an average of 48–56 sweeps. In this and subsequent figures where nonnormalized fluorescence traces are shown, the arrow indicates the direction of an increase in fluorescence. (*C*) G-V (*black*) and F-V (*green*) curves for the SPARC probe and Q-V (*blue*) curve of rSkM1. The red line is the G-V curve of the native rSkM1. Normalized conductance-voltage (G-V) and fluorescence-voltage (F-V) responses were fitted with a two-state Boltzmann function (*solid lines*). The Q-V curve of rSkM1 is the best fit by a two-state Boltzmann function at 25°C based on the mean z (apparent total charge displacement: 2.3) and midpoint values (−48 mV) reported in Sheets and Hanck (1999). The midpoint value is −29 mV for both G-Vs and −52 mV for F-V. The z value is 6.0 for SPARC G-V, 6.9 for wild-type G-V, and 2.1 for F-V. The dotted black curve is the fourth root of the G-V curve of the SPARC construct for comparison. (*D*) Semilogarithmic plots of the data in *C*. For simplicity, the G-V curve of native rSkM1 has been omitted. (*E*) Fluorescence response speed (onset) as a function of membrane voltage. The time constant of fluorescence modulation is plotted against test potential, steps from a holding potential of −120 mV. The values were obtained by a single exponential fit of the rise of the fluorescence change. The solid line is a sigmoidal fit of the data.

upstream fragment and by AscI and BstZ17I for the downstream fragment. The BsiWI/BstZ17I digested rSkM1 in the pSP64T vector was ligated together with the two small fragments to produce the construct with the added AscI site.

EGFP and wild-type GFP flanked by AscI sites were prepared by PCR using the pEGFP plasmid (BD Biosciences Clontech) or humanized wild-type GFP (see above) in zero-blunt vector as a template. The AscI-flanked GFP fragments were further cloned into the AscI site introduced into the channel sequence. The direction of the insert was confirmed by PCR using a primer internal to the GFP sequence (5′-CCACCTACGGCAAGCT-GACC) and a primer upstream of the insertion site (5′-CATCAATCT-GATCCTGGCCGTG). All junctions and PCR-amplified regions were directly confirmed by DNA sequencing (Keck DNA Laboratory at Yale School of Medicine).

In vitro transcription and electrophysiology

After linearizing the construct-containing plasmid by *Sal*I, in vitro transcription was performed using a MEGAscript kit (Ambion, Austin, TX) with a GTP to capGTP ratio of 1:1. The isopropanol-precipitated cRNA was dissolved in nuclease-free water, and diluted to 0.3–0.5 μg/μl before injection. *Xenopus laevis* was maintained according to guidelines established by the National Institutes of Health and the Pierce Laboratory Animal Care and Use Committee. We followed conventional procedures for *Xenopus laevis* oocyte isolation, injection, and incubation (Stuhmer, 1992). A day after separation by collagenase (Gibco BRL, Rockville, MD), each oocyte was injected with 50 nl cRNA solution, then incubated at 17°C in ND96 solution (5 mM HEPES, pH 7.6, 96 mM NaCl, 2 mM KCl, 1.8 mM $CaCl_2$, 1 mM $MgCl_2$) containing penicillin (100 U/ml) and strepto-

mycin (100 μg/ml). Two to 5 days after injection, the oocytes were tested using two-electrode voltage clamping (Warner Instruments, Hamden, CT) in 1 mM dithiothreitol (DTT) containing ND96 solution at room temperature (≈25°C). Electrodes (0.2–1.0 MΩ) were filled with 3 M KCl. For most experiments, depolarizing pulses were applied to oocytes at 1-s intervals.

Optical recording

Oocytes were imaged using a long working distance (3.3 mm), 40× (0.8 NA) water immersion objective (Olympus LUMPlanFI attached to an Olympus BX50WI upright microscope. To measure fluorescence change, the oocytes were epi-illuminated by a 100 W mercury light source using a D390/22 or HQ470/44 exciter filter, a 495 nm long-pass dichroic, and a 500–550 nm emission filter. Interference filters were obtained from Chroma Technology (Brattleboro, VT). The fluorescence light was focused onto a H7732–10 photomultiplier module (Hamamatsu Photonics, Bridgewater, NJ) by a 32-mm collector lens (Edmund Scientific, tonawanda, NY) and the signals were filtered at 1 kHz (8-pole Bessel filter, Frequency Devices, Haverhill, MA) before digitization at 10 kHz by a 16-bit analog-to-digital converter card (National Instruments, Austin, TX). Fluorescence, current, and voltage traces were acquired by software written using LabView (National Instruments).

Data analysis

Analysis of data and curve fitting were performed using macros written in Igor Pro (WaveMetrics, Lake Oswego, OR). The leak and capacitive current were subtracted by the P/4 protocol (Armstrong and Bezanilla, 1977). The total charge displacement (z) and midpoint ($E_{1/2}$) values were determined by curve fits of the data to a two-state Boltzmann function (Hille, 1992). The F in $\Delta F/F$ was corrected for the high intrinsic fluorescence of oocytes by averaging the fluorescence of five uninjected oocytes recorded the same day. Approximately 1/4 to 1/6 of the total fluorescence was derived from the yolk.

RESULTS

Design of constructs

Sodium channels offer several advantages over potassium channels for studies seeking to create an optical probe that will report rapid gating and conformational changes. First, sodium channels form a functional channel from a single polypeptide chain (α subunit) whereas potassium channels are formed from homo- or heterotetramers of a single domain (Armstrong and Hille, 1998; Isacoff et al., 1990; Marban et al., 1998). This structural difference allows targeting of an optical reporter to a specific interdomain region. In addition, because a recombinant sodium channel will not assemble with native sodium channel α subunits, the expression of a nonconducting mutant channel will have less effect on native sodium conductances.

We used a sodium channel mutant that contains two extracellular cysteines that, under normal conditions, form a disulfide bond that occludes the channel pore (Benitah et al., 1997). Upon the addition of a reducing agent (i.e., DTT) to the extracellular solution, this bond is broken, the pore becomes unobstructed, and the channel conducts normally, although gating movements are likely intact. The use of this mutant channel allowed us to express the channel in a nonconducting form, but still measure currents after reversibly reducing the disulfide bond.

In designing potential probes, we avoided inserting GFP within transmembrane regions to reduce the likelihood of disrupting insertion of the channel into the plasma membrane or altering its normal function. Enhanced GFP (EGFP) (Cormack et al., 1996) was inserted at eight sites within intracellular domains of the channel sequence and at two additional sites in the extracellular loop between the third and fourth (S4) transmembrane segments of domain IV of the channel (Fig. 1 *A*).

Screening of constructs

When expressed in *Xenopus laevis* oocytes, all 10 constructs produced increased membrane fluorescence and most produced voltage-activated inward currents (data not shown). However, only a single insertion site produced membrane fluorescence that was clearly altered by changes in transmembrane potential. In SPARC, GFP was inserted between the second and third domains of the channel (Fig. 1 *A*). Four days after injection of SPARC cRNA, the oocyte's surface exhibited, on average, 4 to 5 times stronger green fluorescence than uninjected oocytes. The fractional change in fluorescence was ~0.5% per 100 mV (Fig. 1 *B*). The fractional change in fluorescence was similar under conducting (with 1 mM DTT) and nonconducting conditions (data not shown). All traces presented below were obtained in the presence of DTT. Expression of the SPARC probe produced peak ionic currents similar in amplitude (5–15 μA/oocyte) to those seen with expression of the wild-type rSkM1 α subunit (Fig. 2 *B*). The conductance-voltage (G-V) curve (Fig. 1 *C*) of SPARC also matches that of the wild-type channel. It seems that introduction of the GFP sequence into the sodium channel at this location did not dramatically affect expression, membrane targeting, or the voltage-dependence of activation. SPARC-expressing oocytes undergo a rapid reduction in fluorescence intensity that is sustained throughout the duration of the voltage step, exhibiting no detectable inactivation of fluorescence modulation during depolarizing steps up to 100 ms in duration (Fig. 1 *B*).

SPARC likely reports gating of the sodium channel

The relationship between the magnitude of the voltage steps and the change in fluorescence (F-V) of SPARC was not linear but sigmoidal and was fit well by a two-state Boltzmann function (Hille, 1992) (Fig. 1 *C*). This F-V curve, however, does not overlap the conductance profile (G-V) of the construct and differs from the G-V curve in two important ways. First, the F-V curve is far less steep than the G-V

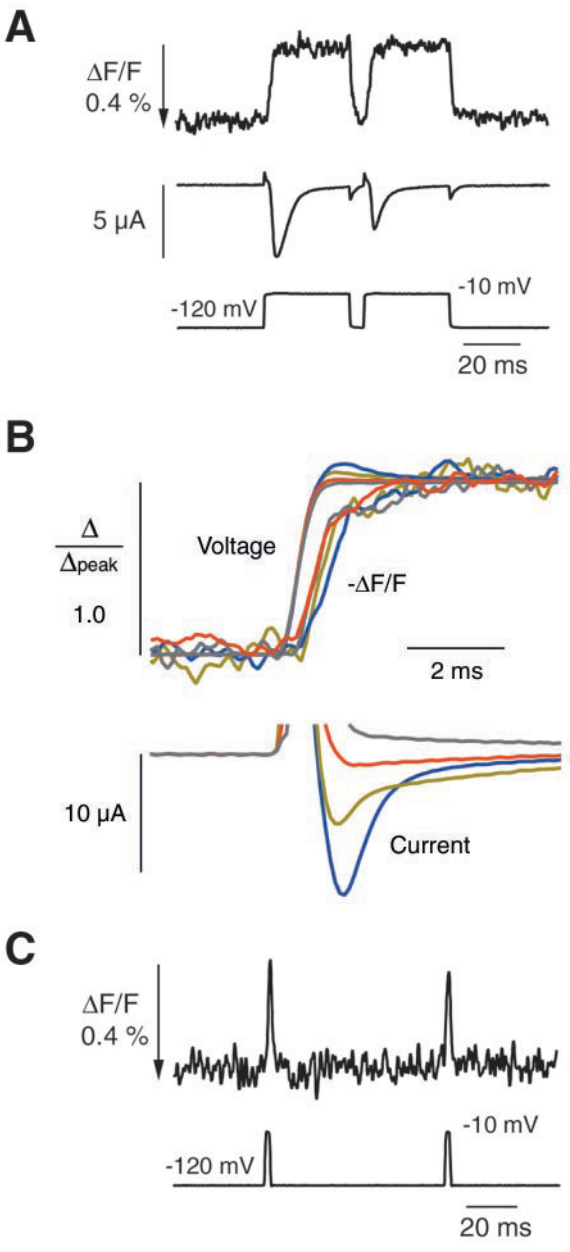

FIGURE 2 Fast fluorescence response of SPARC. (*A*) Detection of two closely spaced depolarizing pulses. The fluorescence change (*top*) is shown in response to two closely spaced (5 ms) 110-mV depolarizing steps. The oocyte potential was held at −120 mV. The middle traces illustrate the ionic current arising during the voltage steps. Note that the fluorescence signal does not inactivate as does the ionic current. The ionic current was leak-subtracted using a P/4 protocol (Armstrong and Bezanilla, 1977). The fluorescence and current traces are averages of 100 sweeps. (*B*) Onset of SPARC response to 100 ms, V_m >−20-mV voltage steps (Fig. 1 *B*) on an expanded time scale. Top: normalized fluorescence response overlaid on normalized voltage steps applied to the oocyte. Bottom: voltage-dependent current. (*C*) Faithful representation of short-duration (2-ms) voltage steps (from −120 to −10 mV). The fluorescence trace is an average of 35 sweeps.

curve (z = 2.1 for F-V vs. $z \approx 6$ for G-V), and second, it is shifted 20 mV (at the midpoint) in the hyperpolarized direction. This negative shift indicates that a significant fraction of fluorescence modulation occurs before the channel opening. In contrast, the F-V curve closely resembles published plots of gating charge movement (Q-V) in the SkM1 channel (Fig. 1, *C* and *D*) (Cha et al., 1999a; Sheets and Hanck, 1999). Moreover, a semilogarithmic transformation of the F-V curve produces a curve with a slope that is very similar to values of the fourth root of the G-V curve (Fig. 1 *D*). Sodium channels have four distinct mobile charged segments (S4) (Marban et al., 1998). Movements of these segments are believed to cause opening (gating) of the channel and can be observed as gating currents (Bezanilla, 2000; Yang et al., 1996; Yang and Horn, 1995). The slope of the G-V curve ($\approx 6\ e_o$) indicates that gating charge movements of all four domains are likely involved in activation gating of sodium channels (Kontis et al., 1997). In contrast, the slope of the F-V curve (2.1 e_o) suggests that the fluorescence change observed arises from the movement of the gating charge in only 1 of the 4 domains. This finding is also similar to characteristics of gating currents (Bezanilla, 2000; Conti and Stuhmer, 1989; Sigworth, 1994).

Although SPARC has a nonlinear fluorescence-voltage relationship, it can still monitor subthreshold membrane potential changes (i.e., postsynaptic potentials in neurons). The F-V profile is less steep (Fig. 1 *C*) between steps to −90 and −20 mV than that seen with the FlaSh construct, where the F-V curve has much steeper voltage dependence (Siegel and Isacoff, 1997).

SPARC's fluorescence change does not inactivate

Sodium channel currents undergo rapid inactivation. The ΔF of SPARC did not inactivate during depolarizations that produced complete inactivation of the sodium channel current (Fig. 2 *A*). The gating charges associated with domains III and IV become immobilized after prolonged depolarizations (Cha et al., 1999a) and are only capable of moving again after extended periods of hyperpolarization. Our findings therefore suggest that the fluorescence response likely arises from movements of gating charge in domains I or II. This hypothesis is also in good agreement with the location of the GFP insert. Antibody binding studies have shown that the first half of the intracellular loop between domains II and III is likely situated under domains I and II (Sun et al., 1995). These observations support the interpretation that gating-related movements in the channel, but not those associated with inactivation, are the principal events associated with the modulation of the fluorescence intensity of SPARC. This is consistent with the speed with which the change in fluorescence arises after the voltage step.

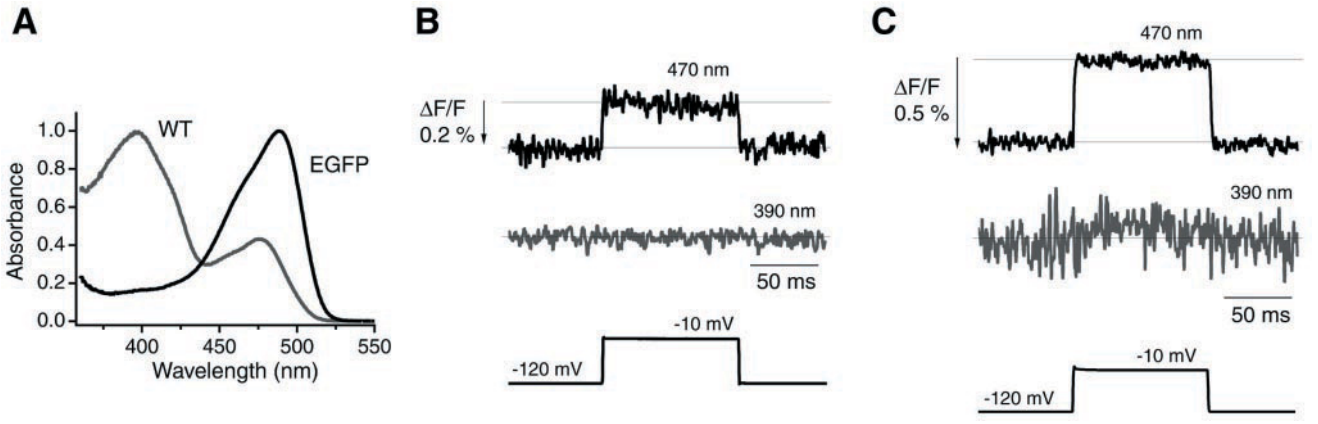

FIGURE 3 Excitation wavelength dependency of the SPARC probe. (*A*) The normalized absorbance spectrum of the EGFP (*black*) and mammalianized wild-type GFP (*gray*) used in SPARC. (*B*) Excitation wavelength-dependent fluorescence modulation of wild-type GFP containing SPARC. A distinct change in fluorescence is observed only with 470-nm centered excitation light (black). Both traces were recorded from the same oocyte and represent averages of 60 sweeps. (*C*) Excitation wavelength-dependent fluorescence modulation of EGFP SPARC. A much greater change in fluorescence is observed when the oocyte is excited with 470 nm centered light (*black*) when compared with an oocyte excited by 390-nm centered light (*gray*). Both traces were recorded from the same oocyte and represent averages of 45 sweeps.

SPARC faithfully detects voltage changes with fast kinetics

The rate at which the fluorescence intensity changes in SPARC-expressing oocytes depends on membrane voltage (Fig. 1, *B* and *E*). The change in fluorescence is greatest (τ_{on} $<$0.8 ms) with voltage steps above ~-20 mV. The rate at which the fluorescence intensity relaxed upon repolarization to -120 mV was independent of the magnitude of the depolarizing step (Fig. 1 *B*). The voltage-dependent acceleration of the response likely reflects the τ_m of the sodium channel (Hodgkin and Huxley, 1952).

The speed of the fluorescence signals we have recorded may underestimate the true response time of SPARC because the settling time of our voltage clamp setup is long (350 μs for 10–90% of 100-mV square voltage pulse) (Fig. 2 *B*). However, for large voltage steps ($>$100 mV), the fluorescence change was almost complete before there was detectable ionic current, a result consistent with the ΔF signal being a reporter of gating-charge movement. With such rapid kinetics, the probe was capable of faithfully recording rapid voltage transients similar in amplitude and duration (2 ms) to neuronal action potentials (Fig. 2 *C*). These features of speed and high fidelity indicate that SPARC is a good reporter of conformational changes associated with gating-charge movement.

SPARC's fluorescence change depends on the deprotonated-state of GFP

It is known that the fluorophore of wild-type GFP exists in a protonated and deprotonated state (Brejc et al., 1997) and that these two states absorb (and are excited) at different wavelengths of light (Fig. 3 *A*). We compared the fluorescence response seen when SPARC was excited with 390 nm (protonated form) versus 470 nm (deprotonated form) light in a construct that contained wild-type GFP. The signal-to-noise ratio under 470 nm excitation was lowered because of the smaller fractional changes ($\sim$1/2.5) and the smaller basal fluorescence ($\sim$1/2.5 at 470 nm excitation; data not shown). Although the fluorescence intensity is greater with 390 nm excitation light, we only observed a voltage-dependent change in fluorescence when 470 nm light was used (Fig. 3 *B*). Therefore, it seems that only the deprotonated form of the GFP fluorophore in SPARC undergoes a voltage-dependent change in fluorescence intensity. This finding was confirmed in experiments using an EGFP inserted version of SPARC in which only the deprotonated form of the fluorophore exists (Fig. 3 *A*) (Haupts et al., 1998). The EGFP form of SPARC also exhibited a large voltage-dependent change in fluorescence using 470-nm centered excitation and only a very small change was seen using 390-nm centered excitation light (Fig. 3 *C*). This smaller fractional change in fluorescence with 390 nm excitation is likely attributable to the smaller absorbance cross-section of EGFP (Haupts et al., 1998) (Fig. 3 *A*).

DISCUSSION

Our results demonstrate that SPARC is a self-contained fluorescent voltage indicator. Considering its response speed, distinctive voltage dependence, and lack of inactivation, the fluorescence change of SPARC is likely a direct optical readout of gating-charge movement of the channel. The midpoint value and slope of SPARC's F-V curve agree closely with the corresponding values reported previously for the Q-V curve of the SkM1 sodium channel (Fig. 1, *C*

and *D*) (Cha et al., 1999a; Sheets and Hanck, 1999). The total charge displacement (*z* value) required for SPARC's fluorescence change is 2.1 e_o (Fig. 1, *C* and *D*), a value that is very similar to the single-shot charge (z_g) estimated by similar fitting to the Q-V curve for the sodium channel gating (2.07 $\pm$ 0.25 e_o) (Conti and Stuhmer, 1989). Technical restraints involving the level of sodium channel expression and the settling time of our voltage clamp preclude our directly measuring gating charge movement in oocytes. The midpoint value for the SkM1 sodium channel's Q-V curve is ~ -50 mV (Cha et al., 1999a; Sheets and Hanck, 1999); we obtained -52 mV for the F-V curve of SPARC's fluorescence modulation. Because all four domains are involved in sodium channel activation (Kontis et al., 1997), a simple calculation from *z* value of the G-V curve (Fig. 1 *C*) gives the number of charges displaced per gate as 1.5 e_o (= 6.0/4). This value is a bit smaller than 2 e_o, but is reasonable considering that fitting the G-V curve to the Boltzmann function has been shown to greatly underestimate the total charge displacement involved in channel opening (Hirschberg et al., 1995). Although the real value of *z* for opening of sodium channels is at least 12 charges (Hirschberg et al., 1995), the curve fitting usually gives a value of 4 to 7 total charges (Almers, 1978; Stimers et al., 1985).

Observation of gating charge movement is typically conducted through electrical recordings of gating current. Given the small size of gating current relative to the ionic current (i.e., 1/50 $\sim$ 1/200 of I_{ionic}), recording such currents usually requires suppression of major voltage-dependent ionic current (i.e., by a pore-blocking toxin) (Bezanilla and Stefani, 1998; Sigworth, 1994). Although further studies are required to establish that the fluorescent protein contained in SPARC does not modify gating, SPARC and SPARC-like constructs could possibly be used as a new tool for optical observation of gating-charge movement without modifying the voltage-dependent current. Moreover, because we did not observe difference in the fluorescent signals between conducting and nonconducting SPARC-expressing oocytes, our channel, in which the pore is occluded by the dicysteine-cross-linking, still likely undergoes the conformational rearrangements evoked by gating-charge movement. Therefore, SPARC could also be used as a tool to identify pharmacological and molecular conditions that modify ion channel gating in large-scale screenings.

These results provide a novel approach to monitor rapid and subtle protein movements in vivo. By inserting a fluorescent protein within a larger protein, it is possible to monitor movements in the parent protein's structure on a rapid timescale. Insertion of GFP within the coding sequence of a particular protein has been suggested and tested (Baird et al., 1999; Biondi et al., 1998; Doi and Yanagawa, 1999), but most tagging has been largely limited to appending GFP to the ends of a protein (Gerdes and Kaether, 1996; Marshall et al., 1995; Tsien, 1998). In the case of SPARC, the reversible change in fluorescence intensity resulting from the insertion of GFP between the second and third domain suggests a significant voltage-dependent conformational change in this region of the channel, where previously little motion was thought to occur during channel activation (Catterall, 2000). Insertion of GFP in other locations of rSkM1 did not result in constructs that displayed voltage-dependent fluorescence changes, suggesting that this region of the channel between the second and third domains is involved in a distinctive movement. Given the conserved domain structure of sodium and calcium channels, the strategy described here potentially provides a method for the in vivo study of gating in this entire class of channels. For example, the introduction of GFP by homologous recombination into the gene encoding presynaptic calcium channels could potentially allow observation of synaptic activity in intact and semi-intact preparations.

The fluorescence modulation of SPARC suggests new possible uses of GFP. Fluorescence modulations of GFP-tagged constructs are typically produced by changes in the energy transfer from a fluorescent/luminescent donor to an acceptor protein (i.e., FRET) (Miyawaki et al., 1997; Xu et al., 1999), but not usually by single GFP fluorescence modulation, except for some rare cases (Baird et al., 1999; Siegel and Isacoff, 1997). Although FRET is a powerful tool for measuring conformational changes within or between proteins, such approaches require tagging with two fluorophores (Mitra et al., 1996; Miyawaki et al., 1997). Because fluorescent proteins are not small (238 aa in wild-type GFP) (Prasher et al., 1992), the FRET method may not always be suitable for the study of a single protein's movement. SPARC suggests that by attaching GFP to a moving part of a protein, it is possible to monitor conformational rearrangements by following changes in the fluorescence emission of the attached GFP.

Perhaps the most exciting potential use for SPARC is as a genetically encodable probe of cellular electrical activity. By targeting SPARC to particular classes of neurons it may be possible to monitor neuronal activity optically. Although this potential use is unique, SPARC has several limitations when compared with conventional voltage-sensitive dyes (Cohen and Salzberg, 1978; Cohen et al., 1978). First, although the response kinetics of SPARC are far more rapid than those of FlaSh, SPARC is likely not as fast as the voltage-sensitive dyes. For example, voltage-sensitive merocyanine dyes respond to membrane potential changes in less than 2 μs (Salzberg et al., 1993). The fluorescence modulation in SPARC depends on conformational changes triggered by gating-charge movements that necessarily follow voltage changes more slowly (Bezanilla, 2000; Sigworth, 1994). A second difference is the nonlinear response properties of SPARC. Whereas SPARC is only relatively linear over a small range of transmembrane potentials (-90 to -20 mV), externally applied voltage-sensitive dyes have linear response properties over several hundred millivolts (Cohen and Salzberg, 1978; Cohen et al., 1978). Finally,

SPARC is unable to detect hyperpolarizations of the membrane. Although this latter property will not affect SPARC's detection of excitatory potentials, it makes it difficult to examine inhibitory postsynaptic potentials. Introduction of known gating mutations could possibly be used to shift the dynamic range of SPARC to more hyperpolarized potentials (Bezanilla, 2000; Kontis et al., 1997; Sigworth, 1994).

The rapid response kinetics and lack of significant inactivation make SPARC an excellent candidate for such studies in excitable cells. Several additional obstacles will need to be overcome before those studies are viable. These include ensuring that the construct will reach the plasma membrane in mammalian cells in sufficient quantities to produce a measurable signal and showing that SPARC expression does not significantly alter the normal physiology of the cell under study. Toward this end we have begun to express SPARC in neuronal and nonneuronal cells in vitro. The results of these studies should provide critical information for the application of SPARC in excitable cells.

The authors thank Larry Cohen, Fred Sigworth, Thom Hughes, and Jim Howe for discussion and advice; Matt Wachowiak for help in optimizing the optical recording; Richard Rascati and Michael Fritz for mechanical and electrical support; Marc Sato of Hamamatsu Corporation for help with fluorescence detection; Mark Bevensee for help with the fluorometry; and Eduardo Marban for the dicysteine mutated sodium-channel construct used in this study.

REFERENCES

Almers, W. 1978. Gating currents and charge movements in excitable membranes. *Rev. Physiol. Biochem. Pharmacol.* 82:96–190.

Armstrong, C. M., and F. Bezanilla. 1977. Inactivation of the sodium channel. II. Gating current experiments. *J. Gen. Physiol.* 70:567–590.

Armstrong, C. M., and B. Hille. 1998. Voltage-gated ion channels and electrical excitability. *Neuron.* 20:371–380.

Baird, G. S., D. A. Zacharias, and R. Y. Tsien. 1999. Circular permutation and receptor insertion within green fluorescent proteins. *Proc. Natl. Acad. Sci. U.S.A.* 96:11241–11246.

Benitah, J. P., R. Ranjan, T. Yamagishi, M. Janecki, G. F. Tomaselli, and E. Marban. 1997. Molecular motions within the pore of voltage-dependent sodium channels. *Biophys. J.* 73:603–613.

Bezanilla, F. 2000. The voltage sensor in voltage-dependent ion channels. *Physiol. Rev.* 80:555–592.

Bezanilla, F., and E. Stefani. 1998. Gating currents. *Methods Enzymol.* 293:331–352.

Biondi, R. M., P. J. Baehler, C. D. Reymond, and M. Veron. 1998. Random insertion of GFP into the cAMP-dependent protein kinase regulatory subunit from *Dictyostelium discoideum*. *Nucleic Acid. Res.* 26: 4946–4952.

Brejc, K., T. K. Sixma, P. A. Kitts, S. R. Kain, R. Y. Tsien, M. Ormo, and S. J. Remington. 1997. Structural basis for dual excitation and photoisomerization of the *Aequorea victoria* green fluorescent protein. *Proc. Natl. Acad. Sci. U.S.A.* 94:2306–2311.

Catterall, W. A. 2000. From ionic currents to molecular mechanisms: the structure and function of voltage-gated sodium channels. *Neuron.* 26: 13–25.

Cha, A., P. C. Ruben, A. L., Jr.George, E. Fujimoto, and F. Bezanilla. 1999a. Voltage sensors in domains III and IV, but not I and II, are immobilized by Na^+ channel fast inactivation. *Neuron.* 22:73–87.

Cha, A., G. E. Snyder, P. R. Selvin, and F. Bezanilla. 1999b. Atomic scale movement of the voltage-sensing region in a potassium channel measured via spectroscopy. *Nature.* 402:809–813.

Cohen, L. B., and B. M. Salzberg. 1978. Optical measurement of membrane potential. *Rev. Physiol. Biochem. Pharmacol.* 83:35–88.

Cohen, L. B., B. M. Salzberg, and A. Grinvald. 1978. Optical methods for monitoring neuron activity. *Annu. Rev. Neurosci.* 1:171–182.

Conti, F., and W. Stuhmer. 1989. Quantal charge redistributions accompanying the structural transitions of sodium channels. *Eur. Biophys. J.* 17:53–59.

Cormack, B. P., R. H. Valdivia, and S. Falkow. 1996. FACS-optimized mutants of the green fluorescent protein (GFP). *Gene.* 173:33–38.

Doi, N., and H. Yanagawa. 1999. Design of generic biosensors based on green fluorescent proteins with allosteric sites by directed evolution. *FEBS Lett.* 453:305–307.

Gerdes, H. H., and C. Kaether. 1996. Green fluorescent protein: applications in cell biology. *FEBS Lett.* 389:44–47.

Glauner, K. S., L. M. Mannuzzu, C. S. Gandhi, and E. Y. Isacoff. 1999. Spectroscopic mapping of voltage sensor movement in the Shaker potassium channel. *Nature.* 402:813–817.

Haupts, U., S. Maiti, P. Schwille, and W. W. Webb. 1998. Dynamics of fluorescence fluctuations in green fluorescent protein observed by fluorescence correlation spectroscopy. *Proc. Natl. Acad. Sci. U.S.A.* 95: 13573–13578.

Hille, B. 1992. Ionic Channels of Excitable Membranes, Second Edition. Sunderland, MA: Sinauer Associates Inc. 54–57

Hirschberg, B., A. Rovner, M. Lieberman, and J. Patlak. 1995. Transfer of twelve charges is needed to open skeletal muscle Na^+ channels. *J. Gen. Physiol.* 106:1053–1068.

Hodgkin, A. L., and A. F. Huxley. 1952. A quantitative description of membrane current and its application to conduction and excitation in nerve. *J. Physiol.* 117:500–544.

Isacoff, E. Y., Y. N. Jan, and L. Y. Jan. 1990. Evidence for the formation of heteromultimeric potassium channels in *Xenopus* oocytes. *Nature.* 345:530–534.

Kontis, K. J., A. Rounaghi, and A. L. Goldin. 1997. Sodium channel activation gating is affected by substitutions of voltage sensor positive charges in all four domains. *J. Gen. Physiol.* 110:391–401.

Marban, E., T. Yamagishi, and G. F. Tomaselli. 1998. Structure and function of voltage-gated sodium channels. *J. Physiol.* 508:647–657.

Marshall, J., R. Molloy, G. W. Moss, J. R. Howe, and T. E. Hughes. 1995. The jellyfish green fluorescent protein: a new tool for studying ion channel expression and function. *Neuron.* 14:211–215.

Mitra, R. D., C. M. Silva, and D. C. Youvan. 1996. Fluorescence resonance energy transfer between blue-emitting and red-shifted excitation derivatives of the green fluorescent protein. *Gene.* 173:13–17.

Miyawaki, A., J. Llopis, R. Heim, J. M. McCaffery, J. A. Adams, M. Ikura, and R. Y. Tsien. 1997. Fluorescent indicators for Ca^{2+} based on green fluorescent proteins and calmodulin. *Nature.* 388:882–887.

Perez-Garcia, M. T., N. Chiamvimonvat, R. Ranjan, J. R. Balser, G. F. Tomaselli, and E. Marban. 1997. Mechanisms of sodium/calcium selectivity in sodium channels probed by cysteine mutagenesis and sulfhydryl modification. *Biophys. J.* 72:989–996.

Prasher, D. C., V. K. Eckenrode, W. W. Ward, F. G. Prendergast, and M. J. Cormier. 1992. Primary structure of the *Aequorea victoria* green-fluorescent protein. *Gene.* 111:229–233.

Salzberg, B. M., A. L. Obaid, and F. Bezanilla. 1993. Microsecond response of a voltage-sensitive merocyanine dye: fast voltage-clamp measurements on squid giant axon. *Jpn. J. Physiol.* 43(Suppl):S37—S41.

Sheets, M. F., and D. A. Hanck. 1999. Gating of skeletal and cardiac muscle sodium channels in mammalian cells. *J. Physiol.* 514:425–436.

Siegel, M. S., and E. Y. Isacoff. 1997. A genetically encoded optical probe of membrane voltage. *Neuron.* 19:735–741.

Sigworth, F. J. 1994. Voltage gating of ion channels. *Q. Rev. Biophys.* 27:1–40.

Stimers, J. R., F. Bezanilla, and R. E. Taylor. 1985. Sodium channel activation in the squid giant axon. Steady state properties. *J. Gen. Physiol.* 85:65–82.

Stuhmer W. 1992. Electrophysiological recording from *Xenopus* oocytes. *Methods Enzymol.* 207:319–339.

Sun, W., R. L. Barchi, and S. A. Cohen. 1995. Probing sodium channel cytoplasmic domain structure. Evidence for the interaction of the rSkM1 amino and carboxyl termini. *J. Biol. Chem.* 270:22271–22276.

Tsien, R. Y. 1998. The green fluorescent protein. *Annu. Rev. Biochem.* 67:509–544.

Ward, W. W. 1998. Biochemical and physical properties of green fluorescent protein. In: Green Fluorescent Protein. Chalfie M and Kain S, editors. Wiley-Liss, New York. 45–75.

Xu, Y., D. W. Piston, and C. H. Johnson. 1999. A bioluminescence resonance energy transfer (BRET) system: application to interacting circadian clock proteins. *Proc. Natl. Acad. Sci. U.S.A.* 96:151–156.

Yang, N., A. L., Jr.George, and R. Horn. 1996. Molecular basis of charge movement in voltage-gated sodium channels. *Neuron.* 16:113–122.

Yang, N., and R. Horn. 1995. Evidence for voltage-dependent S4 movement in sodium channels. *Neuron.* 15:213–218.